Pressure-Induced Magnetization in FeO: Evidence from Elasticity and Mössbauer Spectroscopy

Anastasia P. Kantor,[1,2] Steven D. Jacobsen,[3,1] Innokenty Yu. Kantor,[1] Leonid S. Dubrovinsky,[1]
Catherine A. McCammon,[1] Hans J. Reichmann,[4] and Igor N. Goncharenko[5]

[1]*Bayerisches Geoinstitut, D-95440 Bayreuth, Germany*
[2]*Department of Crystallography and Crystal Chemistry, Moscow State University, 119992 Moscow, Russia*
[3]*Geophysical Laboratory, Carnegie Institution of Washington, 5251 Broad Branch Road NW, Washington, D.C. 20015, USA*
[4]*Geoforschungszentrum Potsdam, Telegrafenberg, Section 4.1, 14473 Potsdam, Germany*
[5]*Laboratoire Léon Brillouin, CEA-Saclay, 91191 Gif-sur-Yvette Cedex, France*
(Received 7 May 2004; published 16 November 2004)

The complete elastic tensor of $Fe_{0.94}O$ (wüstite) has been determined to 10 GPa using acoustic interferometry at GHz frequencies inside a diamond-anvil cell. The soft mode (C_{44}) elastic constant of FeO is reduced by 20% over the experimental pressure range. An unusual discontinuity in the pressure derivatives of C_{11} and C_{12} at 4.7 ± 0.2 GPa corresponds to the pressure at which the onset of a magnetic ordering transition is observed by high-pressure Mössbauer spectroscopy and neutron powder diffraction. Our new results combined with literature structural high P-T data suggest that there is a magnetic, although still cubic, phase of FeO between ~ 5 and ~ 17 GPa.

The elastic properties of single crystals reflect some aspects of the fundamental interactions between atoms in crystals. Elastic constants and moduli also define the macroscopic mechanical properties of solids by relating stress to strain. In magnetic systems, anomalous behavior of the elastic constants (such as mode softening) ahead of phase transitions often reveals a strong phonon-magnon coupling [1–3]. The iron monoxide $Fe_{1-x}O$ (wüstite) is an important member of the highly correlated transition metal monoxide group including NiO, CoO, and MnO, and is also an end-member component of the (Mg,Fe)O solid solution, the most abundant nonsilicate oxide in the Earth [4]. At ambient conditions wüstite exists in a cubic fcc-based rock-salt structure with a nonstoichiometric formula $Fe_{1-x}O$. Hereafter we use ''FeO'' to denote wüstite except when the composition is explicitly given. Our experiments demonstrate the capability of GHz ultrasonics in the diamond-anvil cell (DAC) to study the full elastic tensor of opaque single crystals under high pressures without the optical limitations of Brillouin scattering [5,6] or impulsive stimulated scattering [7]. This Letter presents the first determination of the full elastic tensor of FeO to high precision at hydrostatic pressures up to 9.6 GPa, and shows that a unique combination of Mössbauer spectroscopy (MS), neutron powder diffraction, and GHz-ultrasonic experiments in the DAC reveals new information about magnetoelastic coupling and structurally hidden phase transformations, which are not accompanied by symmetry or structural changes.

The experiments were made using a newly developed gigahertz ultrasonic interferometer for the DAC [8]. Details of acoustic interferometry and data reduction are given elsewhere [9], but the basic principle is akin to optical interferometry with a highly stable radio-frequency signal generator capable of producing phase-coherent tone bursts at 0.5 to 2.1 GHz. In our experiments compressional (P) waves are generated by a ZnO thin-film transducer (driven by the signal generator) sputtered directly onto a single-crystal Al_2O_3 buffer rod. The P-wave buffer rod is acoustically coupled by a small mechanical force to the table facet of the diamond anvil, and delivered to the sample through the [100]-oriented anvil. Shear (S) waves suitable for the DAC require near-optical wavelengths and cannot be made by traditional piezoelectric transducers. GHz-shear waves are made separately using a new P-to-S conversion buffer rod that transfers elastic waves between P and S upon internal reflection inside a single-crystal yttrium-aluminum garnet buffer rod [8].

A single crystal of FeO was synthesized by the floating zone technique [10], with measured cell parameter of $a = 4.3068(1)$ Å, corresponding to the $Fe_{0.94}O$ composition [11]. After initial ambient pressure experiments [12] with FeO crystals oriented parallel to $\langle 100 \rangle$ and $\langle 111 \rangle$ directions, the samples were polished to thin plates measuring about 40 μm in thickness for high-pressure work. Samples of each orientation measuring about 200 μm in diameter were placed into the preindented hole of a T301 steel gasket, and compressed between 0.5 mm culet diamond anvils in a Merrill-Bassett style DAC [13]. The samples were compressed using a 16:3:1 methanol:ethanol:water mixture as a pressure transmitting medium, along with a few ruby spheres. Pressure was measured using the ruby fluorescence scale [14] with uncertainty ± 0.1 GPa at highest pressure reached in this study (9.6 GPa).

Measured single-crystal travel time data $t_P\langle 100 \rangle$, $t_S\langle 100 \rangle$, and $t_S\langle 111 \rangle$ were converted to sound wave velocities using the calculated sample thickness, determined

initially from ambient pressure velocity measurements [12]. An isothermal equation of state for FeO [15] was used to calculate the change in sample length with pressure. The complete elastic tensor was obtained using the pure-mode solutions to the Christoffel equations [16] and is plotted in Fig. 1. The isotropic adiabatic bulk (K_S) and shear (G) moduli were calculated using the variational approach of Hashin and Strikman [17] and are plotted also in Fig. 1.

Our results are in good agreement with the previous ultrasonic elasticity measurements of wüstite to 3 GPa [15]. In this study we observed a change in slope for both C_{11} and C_{12} elastic constants at 4.7 ± 0.2 GPa (Fig. 1, Table I). We tested and confirmed the reversibility of the anomaly by measuring $t_P\langle 100 \rangle$ on both compression and decompression. The change in slope, observed for isotropic moduli of FeO, is also evident in Fig. 1 and Table I. The reason for this kink is suggested by the results of high-pressure MS studies [18]. At a pressure of 5.0 ± 0.5 GPa we observed the beginning of magnetic ordering in polycrystalline ^{57}Fe-enriched $Fe_{0.94}O$ compressed in a methanol:ethanol hydrostatic pressure transmitting medium. The remarkable coincidence in transition pressures suggests that magnetic ordering in FeO is manifested in changes of elastic properties detected by the high-precision ultrasonic data.

We carried out MS studies of the same powder FeO sample used in the previous MS study with the same methodology as described in [18], but to higher pressures (up to 73 GPa) and using cryogenically loaded Ar as a pressure transmitting medium. Mössbauer spectra of the cubic magnetic and the rhombohedral magnetic phases differ in some ways (Fig. 1 in [19]): The Mössbauer spectrum of the cubic phase consists of a broad magnetic part with unresolved lines and a "paramagnetic" doublet, which persists up to the structural phase transformation at
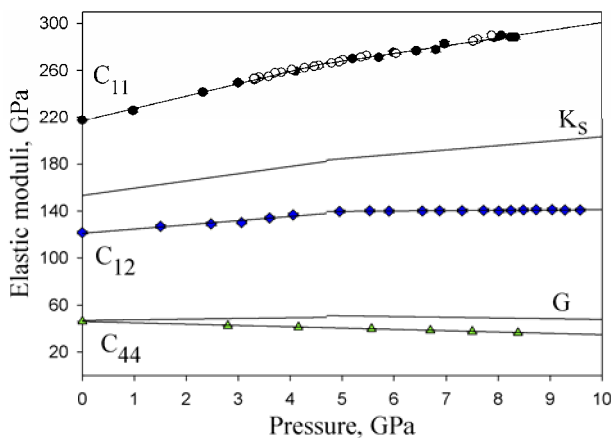
$\sim$17 GPa under hydrostatic conditions [20]. Mössbauer spectra of the rhombohedral phase contain only a relatively well-resolved magnetic sextet. The hyperfine field (B_{HF}) of the magnetic subspectral component changes discontinuously with pressure (Fig. 2) [21]. After a magnetic transition at about 5 GPa B_{HF} increases rapidly with pressure, which is the expected behavior for magnetic ordering transitions. The shape of the magnetization curve between 5 and about 14 GPa (which is the stability field of a AF-IIc structure; see below) suggests saturation at about 25 GPa with B_{HF} equal to about 22 T. Above about 14 GPa wüstite undergoes a rhombohedral transition in an Ar pressure transmitting medium [22] and B_{HF} starts to grow faster and reaches saturation only above 50 GPa with a hyperfine field of about 48 T. We suggest that exchange interactions in the rhombohedral AF-IIr magnetic phase are stronger than in the AF-IIc phase. Also, the paramagnetic doublet that is probably evidence of incomplete magnetic ordering disappears from the Mössbauer spectra of the AF-IIr phase.

In order to obtain independent evidence of magnetic ordering near 5 GPa we performed a high-pressure neutron diffraction study of wüstite at 5 GPa and various temperatures in a sapphire anvil cell. Constant wavelength neutron diffraction (2.7305 Å) measurements were performed at LLB, Saclay, France (a description of the experimental setup and procedure are given in [23]). We observed the magnetic (3/2 1/2 1/2) peak of FeO that appears as a result of a long-range magnetic ordering (Fig. 2 in [19]). The integrated area of this magnetic peak (normalized to the value at 100 K) is plotted as a function of temperature as an inset of Fig. 2. These results confirm that long-range magnetic ordering occurs at 5 GPa and room temperature and support our interpretation of the MS results.

The available experimental and theoretical data are not sufficient to determine the magnetic structure of the FeO cubic phase. However, we can propose a qualitative model of the cubic magnetic structure of FeO that is consistent with experimental observations.

FIG. 1 (color online). The elastic tensor and isotropic adiabatic moduli for $Fe_{0.94}O$. Filled and open circles for C_{11} indicate points measured on compression and decompression, respectively. Lines are linear fits to the data (see Table I).

TABLE I. Coefficients of the linear fits to the elastic moduli of FeO to the equation $A + B * P$ (GPa).

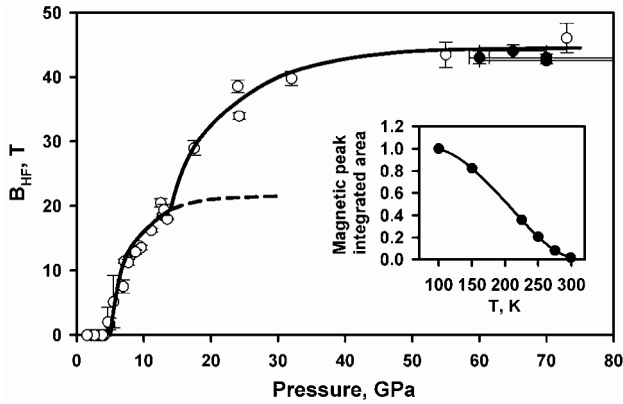| Modulus and pressure range		A	B
C_{11}	$P < 4.7$ GPa	217 ± 1	10.5 ± 0.3
	$4.7 < P < 10$ GPa	234.9 ± 0.5	6.6 ± 0.2
C_{12}	$P < 4.7$ GPa	121 ± 1	3.5 ± 0.7
	$4.7 < P < 10$ GPa	138.4 ± 0.5	0.27 ± 0.7
C_{44}	$0 < P < 10$ GPa	45.9 ± 0.7	-1.13 ± 0.03
K_S	$P < 4.7$ GPa	153 ± 1	6.1 ± 0.4
	$4.7 < P < 10$ GPa	165 ± 1	3.7 ± 0.3
G	$P < 4.7$ GPa	46.8 ± 0.4	0.6 ± 0.1
	$4.7 < P < 10$ GPa	49 ± 1	-0.22 ± 0.03

FIG. 2. Magnetic hyperfine field of $Fe_{0.94}O$ wüstite as a function of pressure (see text for details). Open circles, this study; solid circles, data from Pasternak *et al.* [21]. Inset: integrated area of a magnetic (3/2 1/2 1/2) peak obtained from a neutron diffraction study of wüstite at 5.0(2) GPa (lines are given as guides for the eye). The beginning of long-range magnetic ordering at 5 GPa and room temperature coincide with the transition point obtained from MS studies and elasticity measurements.

At ambient pressure and low temperatures FeO is known to be a type-II antiferromagnet (AF-II) with a crystal structure that has rhombohedral symmetry [24]. According to random-phase Green's-function theory for AF-II fcc structures, spin-phonon interactions result in changes of the interaxial angle (α) and cell dimensions (a) [25,26]. Namely,

$$\Delta\alpha = Nz_1 J_1 \varepsilon_1 (\langle S_i \cdot S_j \rangle_{nn^p} - \langle S_i \cdot S_j \rangle_{nn^a})/24C_{44}, \quad (1)$$

$$\delta a/a = Nz_2 J_2 \varepsilon_2 \langle S_i \cdot S_j \rangle_{nnn^a}/6(C_{11} + 2C_{12}), \quad (2)$$

where α is the rhombohedral setting interaxial angle ($\alpha = 60$ for the cubic structure), N is the number of spins in the system, z_1 ($=12$) and z_2 ($=6$) are the number of nearest-neighbor (nn) and next-nearest-neighbor (nnn) metal ions, $\langle \cdots \rangle_{nn^p}$, $\langle \cdots \rangle_{nn^a}$, and $\langle \cdots \rangle_{nnn^a}$ refer to the thermal averages over parallel nn, antiparallel nn, and antiparallel nnn, respectively, J_1 and J_2 are nn and nnn exchange interactions, $\varepsilon_1 = -r(\partial \ln J_1)/\partial r$ and $\varepsilon_2 = -r(\partial \ln J_2)/\partial r$, r is interspin distance, and finally C_{11}, C_{12}, and C_{44} are the appropriate (cubic) elastic constants.

Equation (2) implies that in AF-II structures, nnn interactions are coupled with changes in C_{11}, C_{12}, and volume striction. It is reasonable to assume that a cubic antiferromagnetic structure of FeO exists (at room temperature and pressures between ~ 5 and ~ 17 GPa), and that in a cubic magnetic structure the nnn interactions are the same as in the rhombohedral AF-II structure. Since C_{44} changes smoothly and continuously up to 9 GPa and $\Delta\alpha = 0$ in this pressure range [20], the nn spin distribution in the cubic magnetic phase of FeO is not equal to that in the classical AF-II structure.
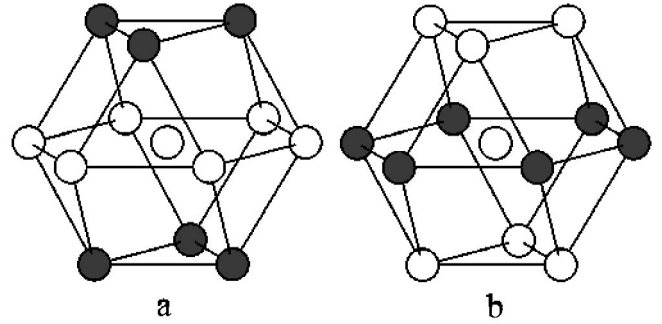

FIG. 3. Nearest-neighbor environment of the metal ion in the (a) AF-IIr and (b) AF-IIc structures. Ions with "+" spins are represented by open circles and ions with "−" spins are shown by filled circles. The cubic $\langle 111 \rangle$ direction is vertical.

In the classical rhombohedral (AF-IIr) structure the parallel spins form sheets within (111) planes of the lattice, where each adjacent sheet is antiparallel. Magnetic interactions between sheets give rise to a slightly attractive or repulsive force resulting in rhombohedral distortion of the lattice below Néel transition. In the AF-IIr structure, all the next-nearest neighbors are antiparallel, and only half of the nearest neighbors are antiferromagnetically coupled, with the other half being coupled ferromagnetically [27] [Fig. 3(a)]. Assuming nnn interactions (of FeO) the same as in the AF-IIr type, we propose a structure where the spins are distributed in the first cation coordination shell in a different way: six nn with antiparallel spins lie in the same close-packing layer as the central ion, while six nn with parallel spins lie in upper and lower hexagonal layers [Fig. 3(b)]. This antiferromagnetic structure (AF-IIc) is closely related to the classical AF-IIr type, but the symmetry remains cubic. Relative to the chemical fcc lattice, the proposed magnetic structure has doubled cell dimensions and a space group $Fd\bar{3}m$, while the crystallographic space group remains $Fm\bar{3}m$. The AF-IIc structure can be considered as an intermediate step towards the AF-IIr structure since every hexagonal layer consists primarily of ions with parallel spins with only one quarter of the ions having antiparallel spins.

In summary, we have determined the complete third-order elastic tensor (C_{ij}) of $Fe_{0.94}O$ to 9.6 GPa using gigahertz ultrasonic interferometry in the DAC. We monitored with high precision a pressure-induced mode softening of the C_{44} elastic constant by 20% over the experimental pressure range, consistent with previous ultrasonic measurements to 3 GPa [15]. An unusual discontinuity in the pressure derivatives of C_{11} and C_{12} at 4.7 ± 0.2 GPa is consistent with the pressure at which magnetic ordering starts, as observed by high-pressure MS in a ^{57}Fe-enriched sample of $Fe_{0.94}O$ and neutron diffraction studies. The results indicate that an intermediate partially magnetic but still cubic phase of FeO exists

at room temperature and in the pressure range from ~ 5 to ~ 17 GPa.

[1] B. Lüthi, T. J. Moran, and R. J. Pollina, J. Phys. Chem. Solids **31**, 1741 (1970).
[2] V.V. Struzhkin *et al.*, Phys. Rev. Lett. **87**, 255501 (2001).
[3] S. Klotz, Z. Kristallogr. **216**, 420 (2001).
[4] S. H. Shim *et al.*, Science **293**, 2437 (2001).
[5] S.V. Sinogeikin and J. D. Bass, Phys. Earth Planet. Int. **120**, 43 (2000).
[6] C. S. Zha, H. K. Mao, and R. J. Hemley, Proc. Natl. Acad. Sci. U.S.A. **97**, 13 494 (1999).
[7] E. H. Abramson, J. M. Brown, and L. J. Slutsky, Annu. Rev. Phys. Chem. **50**, 279 (1999).
[8] S. D. Jacobsen *et al.*, Proc. Natl. Acad. Sci. U.S.A. **101**, 5867 (2004).
[9] H. A. Spetzler *et al.*, Pure Appl. Geophys. **141**, 341 (1993).
[10] J. Berthon *et al.*, J. Cryst. Growth **47**, 736 (1979).
[11] C. A. McCammon and L.-g. Liu, Phys. Chem. Miner. **10**, 106 (1984). The wüstite composition is determined by $a = 3.856 + 0.478y$, where a is the cell parameter in angstroms and y is the Fe/O ratio.
[12] S. D. Jacobsen *et al.*, J. Geophys. Res. **107**, 2037 (2002).
[13] N. Dubrovinskaia and L. Dubrovinsky, Rev. Sci. Instrum. **74**, 3433 (2003).
[14] H. K. Mao, J. Xu, and P. M. Bell, J. Geophys. Res. **91**, 4673 (1986).
[15] I. Jackson *et al.*, J. Geophys. Res. **95**, 21 671 (1990). Birch Murnagham's equation of state for FeO: $K = 154.8(2)$ GPa, $K' = 5.06(6)$ GPa.
[16] K. Brugger, J. Appl. Phys. **36**, 759 (1965).
[17] Z. Hashin and S. Strikman, J. Mech. Phys. Solids **10**, 343 (1962).
[18] I.Y. Kantor, C. A. McCammon, and L. S. Dubrovinsky, J. Alloys Compd. **376**, 5 (2004).
[19] See EPAPS Document No. E-PRLTAO-93-028446 for selected Mössbauer spectra of $Fe_{0.94}O$ and neutron diffraction patterns. A direct link to this document may be found in the online article's HTML reference section. The document may also be reached via the EPAPS homepage (http://www.aip.org/pubservs/epaps.html) or from ftp.aip.org in the directory /epaps/. See the EPAPS homepage for more information.
[20] H. K. Mao *et al.*, Phys. Earth Planet. Int. **96**, 135 (1996).
[21] M. P. Pasternak *et al.*, Phys. Rev. Lett. **79**, 5046 (1997).
[22] L. Dubrovinsky *et al.*, Mater. Sci. Eng. A **288**, 187 (2000).
[23] I. N. Goncharenko, High Press. Res. **24**, 193 (2004).
[24] C. G. Shull, W. A. Strauser, and E. O. Wollan, Phys. Rev. **83**, 333 (1951).
[25] B. Morosin, Phys. Rev. B **1**, 236 (1970).
[26] D. S. Rodbell and J. Owen, J. Appl. Phys. **35**, 1002 (1964).
[27] R. S. Tebble and D. J. Craik, *Magnetic Materials* (Wiley-Interscience, New York, 1969).